

Electronic Supplementary Information for

Ultra-low Power $\text{Hf}_{0.5}\text{Zr}_{0.5}\text{O}_2$ based Ferroelectric Tunnel Junction Synapses for Hardware Neural Network Applications

Lin Chen^{a}, Tian-Yu Wang^a, Ya-Wei Dai^a, Ming-Yang Cha^a, Hao Zhu^a, Qing-Qing Sun^{a*}, Shi-Jin
Ding^a, Peng Zhou^a, Leon Chua^b, and David Wei Zhang^a*

^aState Key Laboratory of ASIC and System, School of Microelectronics, Fudan University,
Shanghai 200433, China

^bDepartment of Electrical Engineering and Computer Sciences, University of California, Berkeley,
CA 94720, USA

* E-mail : linchen@fudan.edu.cn; qqsun@fudan.edu.cn;

The fabrication process is schematically demonstrated in **Fig. S1** in supporting information. Firstly, multiple SiO₂(30 nm)/Pt(50 nm)/Ti stack layers were deposited onto the cleaned SiO₂/Si substrate. 5 nm thickness Titanium is using as an adhesion layer. Pattern and dry etching were applied to form a vertical pillar structure. 9 nm HZO film was then deposited on the pillar sidewall by ALD method. Next, top and bottom contact were etched. 60 nm TiN vertical electrodes were deposited by PVD methods followed by a lift-off process. Finally, samples were annealed in N₂ atmosphere at 450 °C for 30s.

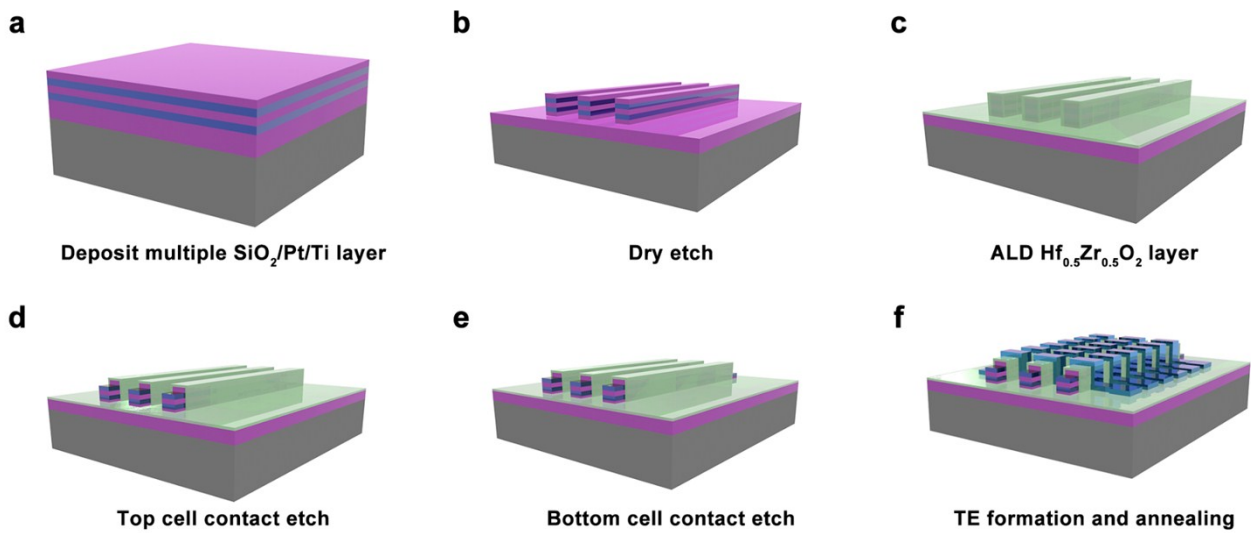


Fig. S1 The fabrication process of HZO-based FTJ array. (a) Multiple SiO₂(30 nm)/Pt(50 nm)/Ti stack layers were deposited onto the cleaned SiO₂/Si substrate. 5 nm thickness Titanium is using as an adhesion layer. (b) Vertical pillar structure formation by pattern and dry etch method. (c) ALD 9 nm HZO thin film on the pillar sidewall. (d) Top contact formation. (e) Bottom contact formation. (f) PVD 60 nm TiN vertical electrodes followed by a lift-off process, then samples were annealed in N₂ atmosphere at 450°C for 30s.

Ferroelectric (FE) HZO-based FTJ exhibits great advantages in nonvolatile memory application. The resistance switching characteristics are derived from electron tunneling across FE HZO layer, which is crucially distinct from oxide-based RRAM. Electrical measurements are performed without any electrical forming process; the conductance ratio is lower than its counterpart, and energy consumption is much lower than that of RRAM under the same device dimension. **Fig. S2** illustrates the energy bandgap diagram of FE-HZO based FTJ under bipolar operation. The electric-field-induced polarization reversal in FE-HZO layer change the conductance of the FTJ.

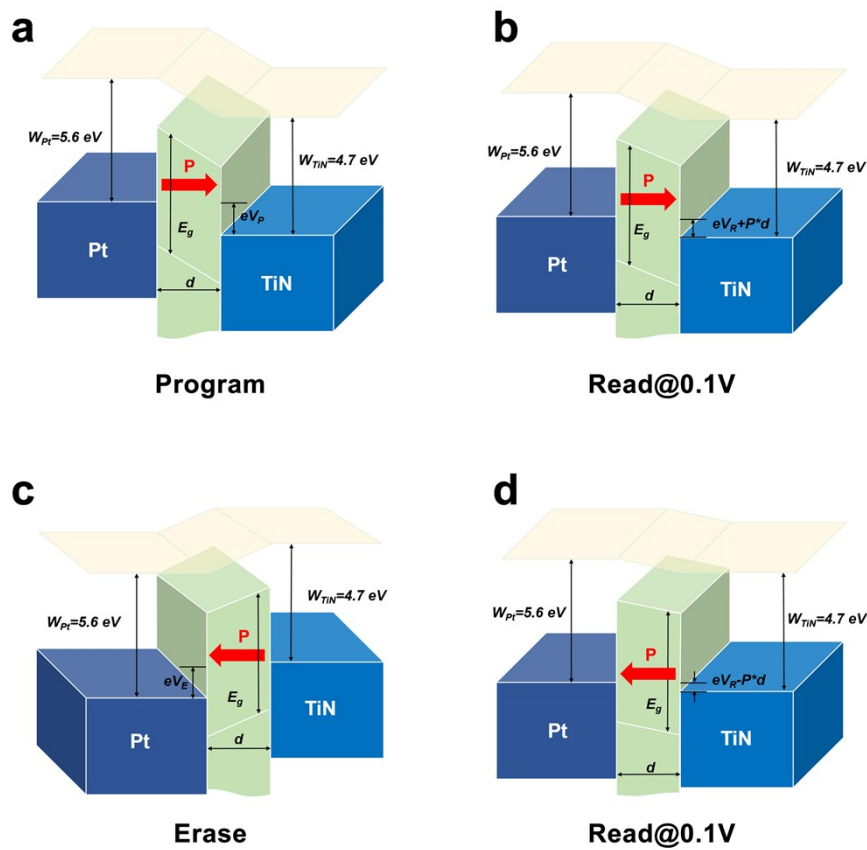


Fig. S2 Energy bandgap diagram of FE-HZO based FTJ under bipolar operation. (a) 6V pulse is applied on the TiN TE to program the FTJ to an ON state. (b) 0.1V read pulse to read the FTJ's state. (c) -6V erase pulse is applied to switch the FTJ to OFF state. (d) 0.1V read pulse to read the FTJ's state.

To estimate the neural network's generalization ability, computer simulation of pattern classification is implemented (shown in the main text). **Fig. S3(a)** shows the convergence of network output for the training set, all the 4 training processes from different initial states according with Gaussian distribution with different values of standard deviation ($1 \mu\text{S}$, $1.25 \mu\text{S}$, $1.5 \mu\text{S}$ and $1.75 \mu\text{S}$) exhibit perfect convergence results. Figure S3b shows the detailed synaptic weights distribution in the training evolution. Perfect classification is obtained after training around 20 epochs.

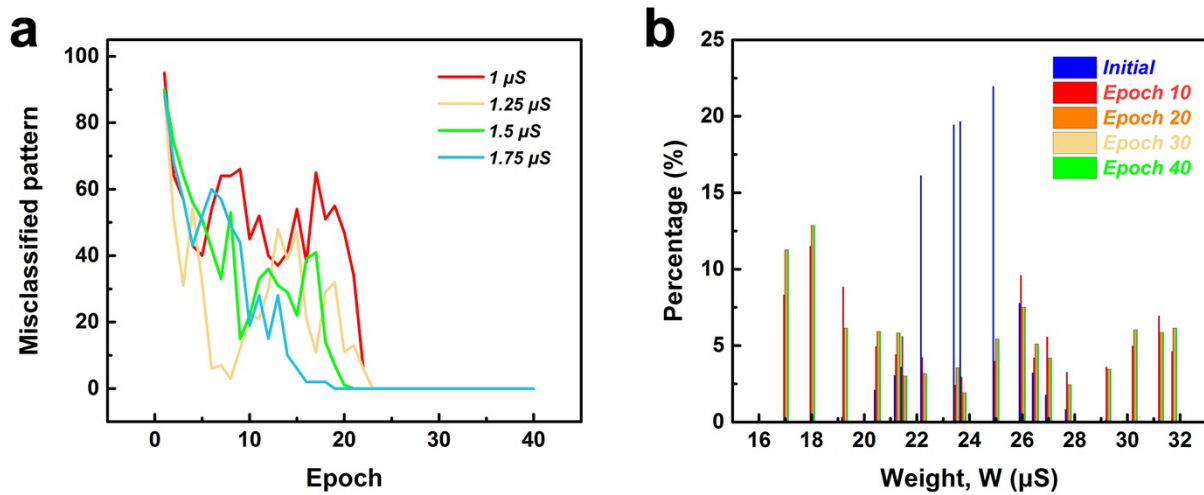


Fig. S3 Simulated implementation of pattern classification and recognition. (a) The convergence of network output for the training set. The corresponding standard deviations of the initial synaptic weights are $1 \mu\text{S}$, $1.25 \mu\text{S}$, $1.5 \mu\text{S}$ and $1.75 \mu\text{S}$. (b) Histogram of synaptic weights at the initial state (with a deviation of $1.5 \mu\text{S}$), measured after training 10 epochs, 20 epochs, 30 epochs and 40 epochs. Perfect classification is achieved after training around 20 epochs.

Table S1. Summary of recent advances of electronic synapses.

Years, Publication	Electronic Synapse system	Switching mechanism	Synaptic function	Energy/power consumption	3D integration	Neuromorphic learning		Accuracy (%)
						Hardwar e	Softwar e	
This work	TiN/FE-HZO/Pt	FE tunneling	Yes	1.8 pJ/spike	Yes	Yes	Yes	96%(simulation)
2015, ^[1] <i>Nature</i>	Ti/Al ₂ O ₃ /TiO _{2-x} /Pt	V _O -filament	-	-	Yes(crossbar)	Yes	Yes	74%(experiment)
2015, ^[2] <i>Adv. Mater.</i>	Pt/WO ₃ /Pt	V _O -filament	Yes	-	No	No	No	-
2015, ^[3] <i>Nat. Mater.</i>	Ag/M ₀ O _x /M ₀ S ₂ /Ag	V _O -filament	Yes	10 nW	No	No	No	-
2015, ^[4] <i>Nano lett.</i>	Pd/Ta ₂ O _{5-x} /TaO _y /Pd	V _O -filament	Yes	-	No	No	No	-
2016, ^[5] <i>Nanotechnology</i>	Ta/TaO ₂ /TiO ₂ /Ti	V _O -filament	Yes	18 pJ/spike	Yes	No	Yes	90%(simulation)
2010, ^[6] <i>Nano lett.</i>	Ag:α-Si memristor	-	Yes	1.37 pJ/spike	Yes(crossbar)	No	No	-
2016, ^[7] <i>IEEE Electron Device Lett.</i>	TiN/HfO ₂ /Pt	V _O -filament	-	-	Yes(crossbar)	Yes	No	-
2017, ^[8] <i>Nat. Mater.</i>	SiO _x N _y :Ag device	Ag-filament	Yes	-	No	No	No	-
2014, ^[9] <i>Nano Research</i>	Bi ₂ S ₃ -NNN/FTO	Schottky emission	Yes	150 nJ/spike	No	Yes	No	-
2015, ^[10] <i>IEEE Trans. Electron Devices</i>	1T1R GST-PCM	Phase change	-	-	Yes(crossbar)	No	Yes	82.9%(experiment)
2011, ^[11] <i>Nano lett.</i>	TiN/GST/TiN	Phase change	Yes	50 pJ/spike	No	No	No	-
2016, ^[12] <i>Nat. Nanotech.</i>	GST-PCM	Phase change	Yes	5 pJ/spike	Yes(crossbar)	No	No	-
2014, ^[13] <i>Appl. Phys. Lett.</i>	Co/BTO/LSMO	FE tunneling	Yes	-	No	No	No	-

References

- [1] M. Prezioso, F. Merrikh-Bayat, B. D. Hoskins, G. C. Adam, K. K. Likharev, D. B. Strukov, *Nature* **2015**, 521, 61.
- [2] Z. H. Tan, R. Yang, K. Terabe, X. B. Yin, X. D. Zhang, X. Guo, *Advanced Materials* **2015**, 28.
- [3] A. A. Bessonov, M. N. Kirikova, D. I. Petukhov, M. Allen, T. Ryhanen, M. J. Bailey, *Nature materials* **2015**, 14, 199.
- [4] S. Kim, C. Du, P. Sheridan, W. Ma, S. Choi, W. D. Lu, *Nano letters* **2015**, 15, 2203.
- [5] I. T. Wang, C. C. Chang, L. W. Chiu, T. Chou, T. H. Hou, *Nanotechnology* **2016**, 27.
- [6] S. H. Jo, T. Chang, I. Ebong, B. B. Bhadviya, P. Mazumder, W. Lu, *Nano letters* **2010**, 10, 1297.
- [7] L. Gao, P. Y. Chen, S. Yu, *IEEE Electron Device Letters* **2016**, 37, 870.
- [8] Z. Wang, S. Joshi, S. E. Savel'Ev, H. Jiang, R. Midya, P. Lin, M. Hu, N. Ge, J. P. Strachan, Z. Li, *Nature materials* **2016**.
- [9] Y. Tian, C. Guo, S. Guo, T. Yu, Q. Liu, *Nano Research* **2014**, 7, 953.
- [10] G. W. Burr, R. M. Shelby, S. Sidler, C. D. Nolfo, *IEEE Transactions on Electron Devices* **2015**, 62, 1.
- [11] D. Kuzum, S. Yu, H. S. Wong, *Nanotechnology* **2013**, 24, 382001.
- [12] T. Tuma, A. Pantazi, M. L. Gallo, A. Sebastian, E. Eleftheriou, *Nature Nanotechnology* **2016**, 11, 693.
- [13] Z. Wang, W. Zhao, W. Kang, Y. Zhang, *Applied Physics Letters* **2014**, 104, 053505.